

# Cinder Cone Morphometry and Volume Distribution at Newberry Volcano, Oregon: Implications for Age Relations and Structural Control on Eruptive Process

Stephen B. Taylor, Jeffrey H. Templeton, Denise E.L. Giles, Earth and Physical Sciences Department, Western Oregon University, Monmouth, Oregon 97361, email: [taylor@wou.edu](mailto:taylor@wou.edu)

## 1. ABSTRACT

Newberry Volcano of central Oregon covers greater than 1300 km<sup>2</sup> and is associated with over 400 basaltic cinder cones and fissure vents (Holocene-Late Pleistocene). Digital geologic maps and 10-m USGS DEMs were compiled with 182 single cones selected for morphometric and volume analyses using GIS. This robust data set provides a framework from which to evaluate cone volume distributions and relative ages in the context of erosional degradation models.

Based on visual inspection of DEM-derived shaded relief maps, each cone was qualitatively ranked with a morphology classification ranging from 1 (well defined cone-crater morphology) to 7 (very poorly defined cone-crater morphology). Morphometric measurements include cone height ( $H_c$ ), average cone slope ( $S_c$ ), long-axis diameter ( $D_l$ ), short axis diameter ( $D_s$ ), and height:width ratio ( $H_c/W_c$ , where  $W_c=(D_l+D_s)/2$ ). Individual cone DEMs were extracted and volumes ( $V_c$ ) calculated using a kriging-based algorithm. Average slopes were derived from 10-m elevation nodes contained within cone polygons. Results according to qualitative morphology rank are summarized as follows: (A) Frequency (no.) 1=11, 2=21, 3=10, 4=35, 5=11, 6=35, 7=59; (B) Average  $V_c$  (m<sup>3</sup>) 1= $1.46 \times 10^7$ , 2= $1.53 \times 10^7$ , 3= $1.25 \times 10^7$ , 4= $4.88 \times 10^6$ , 5= $4.65 \times 10^6$ , 6= $3.07 \times 10^6$ , 7= $1.10 \times 10^6$ ; (C) Average  $S_c$  (deg) 1=19.9, 2=18.2, 3=18.1, 4=14.9, 5=14.4, 6=11.9, 7=10.2; (D) Average  $H_c$  (m) 1=132, 2=124, 3=126, 4=76, 5=78, 6=59, 7=50; (E) Average  $H_c/W_c$  1=0.18, 2=0.20, 3=0.19, 4=0.15, 5=0.14, 6=0.13, 7=0.13. Existing cone degradation models demonstrate that with increasing cone age,  $S_c$ ,  $H_c$ , and  $H_c/W_c$  decrease, respectively. Systematic t-tests ( $\alpha=0.05$ ) of these parameters between morphology classes statistically separates cones into two groups: (1) "Morphometric Group I" = ranks 1-3, and (2) "Morphometric Group II" = ranks 4-7. Spatial analysis of cone-volume distributions shows maxima oriented NW-SE, parallel to regional fault trends (Tumalo Fault and Northwest Rift zones).

The above results suggest that there are two distinct age populations of cinder cones at Newberry. Parallel alignment of cone-volume maxima with known fault trends implies that these structures have an important control on eruptive process in the region. This study provides a framework to guide future geomorphic analysis and radiometric age dating of cinder cones at Newberry Volcano.

## 2. INTRODUCTION

Newberry Volcano is located in central Oregon, in close proximity to the cities of Bend and LaPine (Figure 1). With an estimated volume of 450 km<sup>3</sup>, Newberry is one of the largest volcanoes in the contiguous United States. It is an elongated shield that extends 60 km long north-south and 30 km wide east-west; the summit is marked by a caldera that is 7 by 5 km across (Figures 2 and 3) (MacLeod and Sherrod, 1988). This broad shield complex covers greater than 1600 km<sup>2</sup> and is associated with over 400 basaltic cinder cones and fissure vents (Holocene-Late Pleistocene; Jensen 2002) (Figure 2). The large number of cinder cones provides an important geologic framework from which to conduct morphometric analyses, test existing erosional degradation models, and decipher controls on eruptive magnitude and frequency.

This work represents preliminary morphometric and volume analyses of 182 single cinder cones distributed across Newberry Volcano. Data were compiled from digital geologic maps and 10-m DEMs using GIS (Giles and others, 2003). The results are placed in the context of relative age dating and structural control on volcanic process. As population density is rapidly increasing in Bend and surrounding areas (annual avg. growth = 21%; U.S. Census Bureau, 2003), results of this ongoing investigation may have important implications for volcanic hazards assessment (after Sherrod et al., 1997).

## 3. GEOLOGIC SETTING

Newberry Volcano lies at the west end of the High Lava Plains about 65 km east of the Cascade Range (Figure 1). Owing to its location, Newberry displays tectonic and compositional characteristics of the Cascade Range, High Lava Plains, and Basin and Range (MacLeod and others, 1981; MacLeod and Sherrod, 1988). The volcano is also positioned at the younger end of a sequence of rhyolite domes and caldera-forming ash-flow tuffs that decrease in age from 10 m.y. in southeastern Oregon to less than 1 m.y. near the caldera (Figure 1).

Newberry is located in a complex, extensional tectonic setting dominated by Pliocene to Quaternary faults (MacLeod and others, 1981; MacLeod and Sherrod, 1988). Several major fault zones surround and converge near Newberry, including the Brothers fault zone, the Tumalo fault

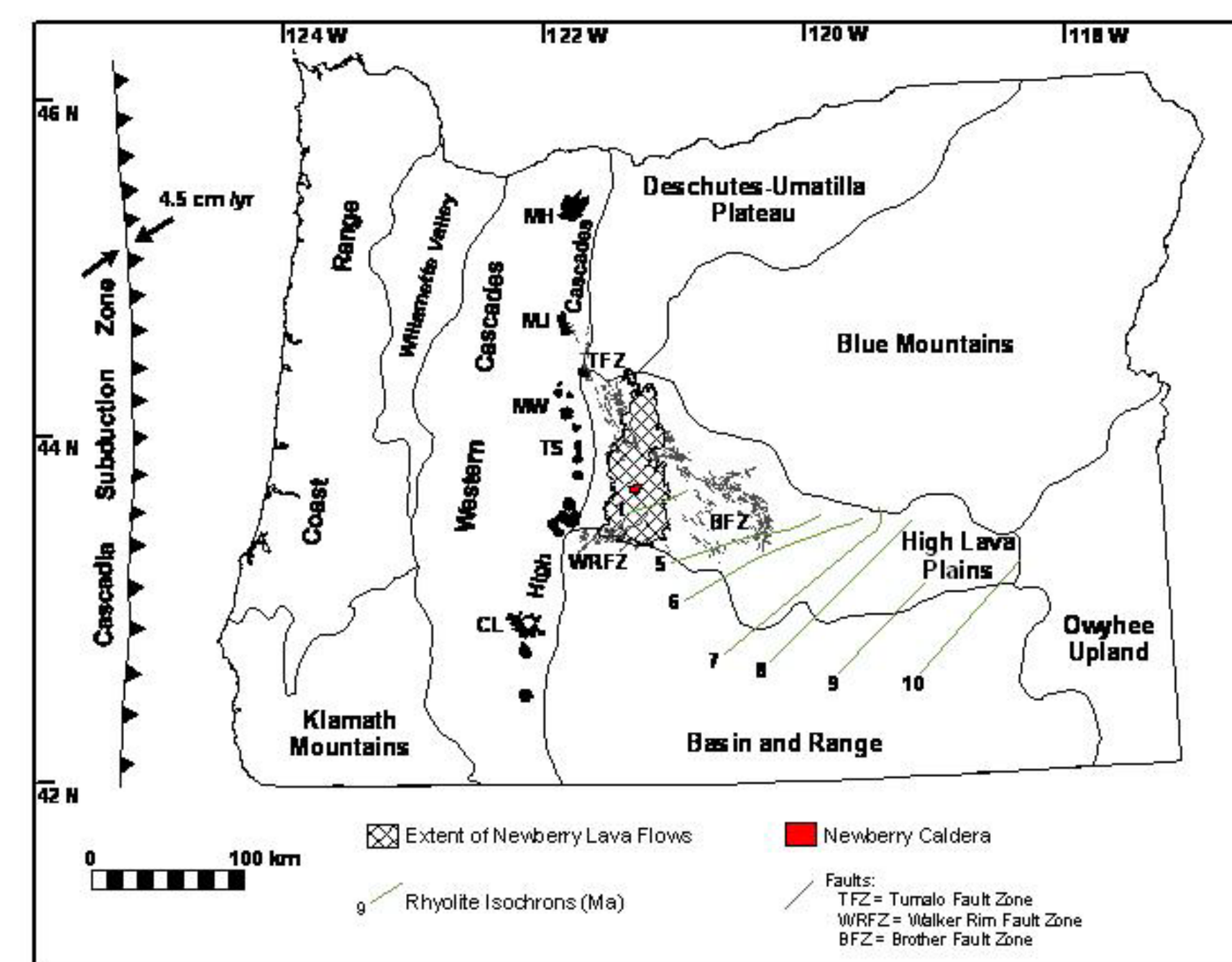


Figure 1. Generalized map of Oregon emphasizing the regional geologic and tectonic framework of Newberry Volcano. Geology after Walker and MacLeod (1991).

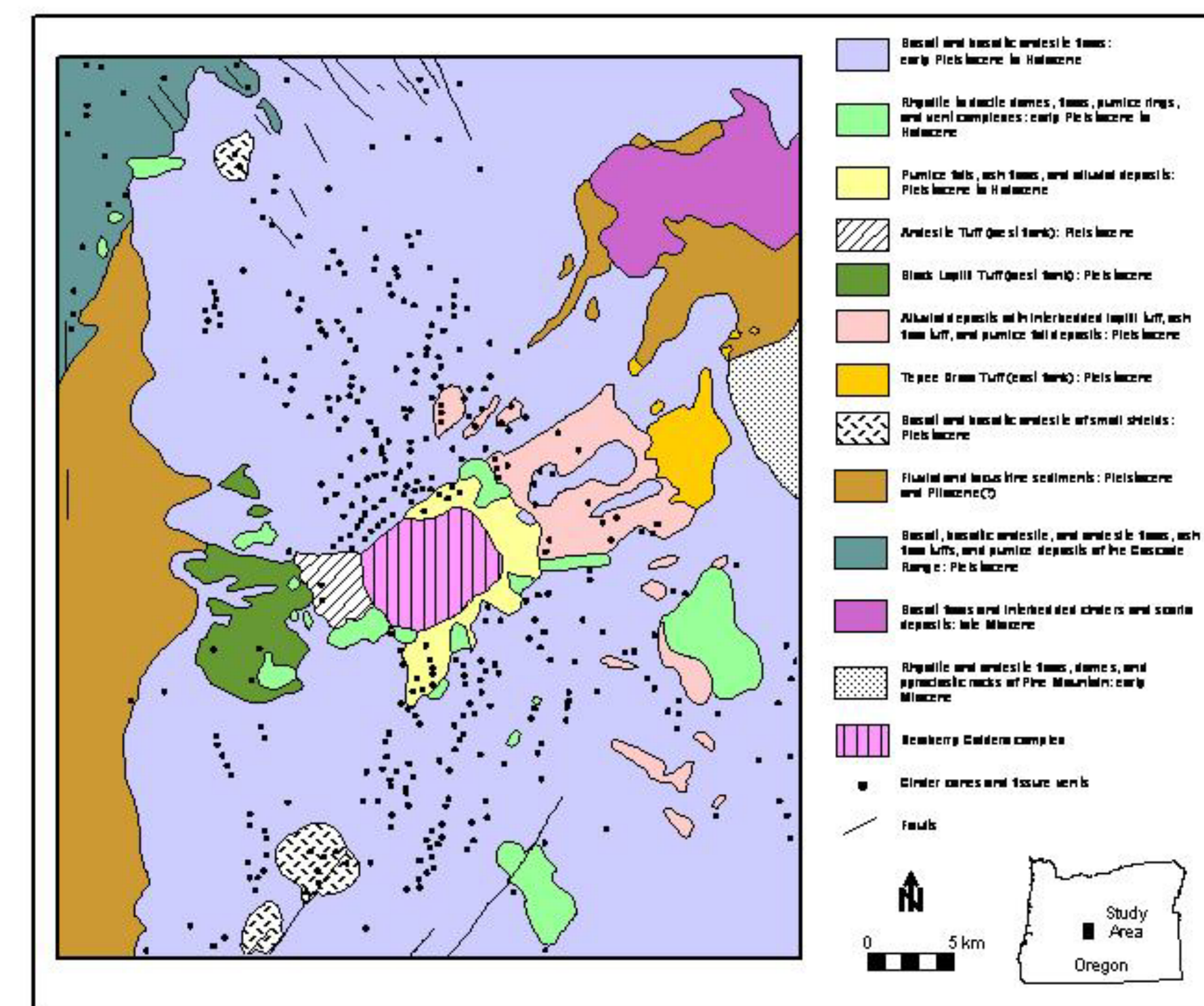


Figure 2. Generalized geologic map of Newberry Volcano (after Jensen, 2000).

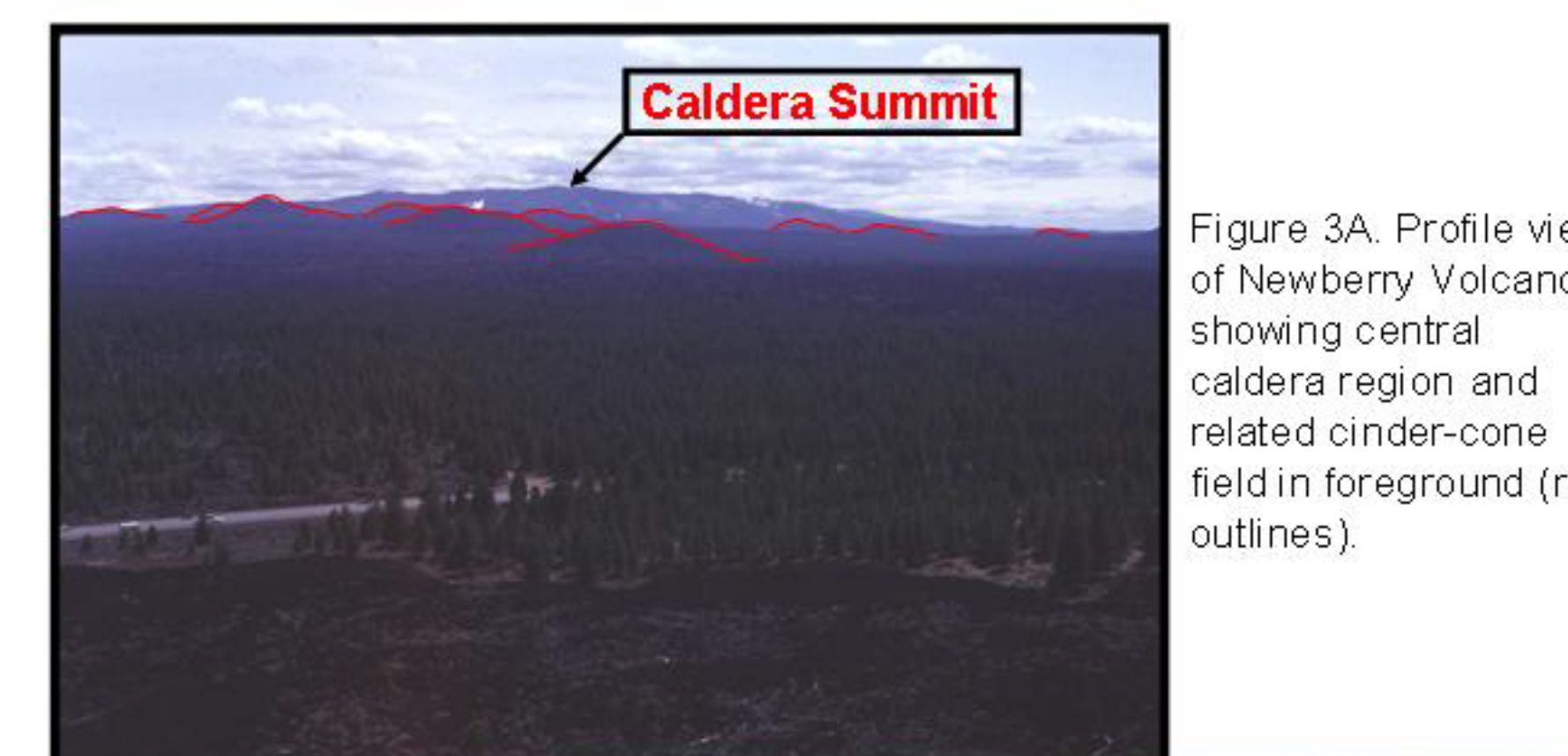


Figure 3A. Profile view of Newberry Volcano showing central caldera region and related cinder-cone field in foreground (red outlines).



3B. Aerial view of Lava Butte cinder cone (6160 +/- 70 C14 yrs) (Sept. 3, 1986, ©R.A. Jensen).

zone, and the Walker Rim fault zone (Figures 1 and 2). The Brothers fault zone is a major west-northwest trending domain of dominantly right-lateral strike slip faults that extend from southeastern Oregon to the northeast flank of Newberry, where the faults are buried by Quaternary lava flows (MacLeod and others, 1981; MacLeod and Sherrod, 1988). The north-northwest trending Tumalo fault zone extends from the east side of the Cascades to the lower northern flanks of Newberry, where older lava flows are offset by this fault system. Along the southern flanks of Newberry, the north-northeast trending Walker Rim fault zone offsets older flows (Figures 1 and 2).

The flanks of Newberry Volcano are covered mostly by basaltic andesite lava flows with subordinate amounts of basalt and andesite lavas (Figure 2). Flow rocks are typically porphyritic with abundant plagioclase phenocrysts and lesser amounts of olivine that resembles basalt, but most are basaltic andesite with SiO<sub>2</sub> values of 54-55 wt.% and compositional characteristics similar to calc-alkaline flows in Cascade Range (MacLeod and Sherrod, 1988). Holocene flow rocks are subdivided relative to the Mazama ash-fall deposits into younger than 6,850 and older than 6,850 (MacLeod and others, 1981). The Mazama pumice deposit, which mantles the area around Newberry with up to 1 m of ash and lapilli, was erupted from Mt. Mazama to form Crater Lake ~6800 years ago (6845 +/- 50 C14 yr B.P.; Bacon, 1983).

Cinder cones and related lava flows are most abundant on the north and south flanks of Newberry, less common on the east flank, and uncommon on the west flank (Figures 2 and 3). Many cones are aligned, and previous workers have identified three broad zones based on these arrays (MacLeod and others, 1981; MacLeod and Sherrod, 1988). On the south flank, the cones display a conspicuous north-northeast trend, co-linear with the Walker Rim fault zone (Figure 2). On the north flank, the cones form a wider north-northwest trending array that parallels the Tumalo fault zone. Some on the north flank also display curved arrangements parallel to caldera walls and are presumably related to local stresses within volcano (MacLeod and Sherrod, 1988) (Figure 2). MacLeod and Sherrod (1988) interpreted the cone and vent alignments to represent the surface expression of dikes at depth that formed in response to regional stress fields. They observed that the apparent curvilinear distribution of cinder cones and fissure vents on the north and south flanks of Newberry trend mostly parallel to the Walker Rim and Tumalo fault zones, suggesting that these fault zones form a single arc-shaped fault zone beneath Newberry. MacLeod and Sherrod (1988) also suggested that north-northwest trending cones and fissure vents are relatively younger than those trending north-northeast. The work presented herein provides a quantitative framework from which to evaluate this interpretation.

## 4. METHODOLOGY

A select set of Newberry cinder cones (n = 182) were analyzed by measuring a suite of morphometric parameters that are commonly used to quantitatively characterize shape, eruptive volume, and relative age. Data sources included a digitized version of the published Newberry geologic map (1:62,500; MacLeod and others, 1995; Giles and others, 2003), USGS 10-m digital elevation models (DEM), and 1:24000 digital orthophotoquads (DOQ). The sample population was selected on the basis of the following criteria: (1) basaltic cinder cones mapped as "C<sub>c</sub>" by MacLeod and others (1995), (2) single cones that are not part of a fissure-vent system, (3) intact cones that do not appear to be topographically breached, (4) exposed cones that are not significantly covered by younger lava flows, and (5) cones that are clearly separated from nearest neighbors (e.g. Lava Butte, Figure 3B).

Individual cone DEMs were extracted from the USGS 10-m quadrangles and analyzed using a suite of GIS-related software including ArcView (ESRI), ArcGIS (ESRI), Idrisi (Clark Labs), Cartalynx (Clark Labs), and Surfer (Golden Software). Based on visual inspection of DEM-derived shaded relief maps, each cone was qualitatively ranked with a morphology classification ranging from 1 (well defined cone-crater morphology) to 7 (very poorly defined cone-crater morphology) (Table 1, Figure 4). Morphometric techniques were modified from those developed by Scott and Trask (1971), Porter (1972), and Wood (1980). Parameters include cone height ( $H_c$ ), average cone slope ( $S_c$ ), long-axis diameter ( $D_l$ ), short axis diameter ( $D_s$ ), and height:width ratio ( $H_c/W_c$ , where  $W_c=(D_l+D_s)/2$ ). Long and short axes ( $D_l$  and  $D_s$ , respectively) were digitized from cone polygon outlines as defined by unit C<sub>c</sub> from MacLeod and others (1995). Cone height and slope were derived from 10-m elevation nodes contained within C<sub>c</sub> polygons. Finally, cone volumes were calculated from the DEMs by clipping the edifice footprint (2x the cone-bounding rectangle), masking the cone relief to zero, and re-gridding the "masked" cone using a kriging-based algorithm (Figure 5). Cone volumes ( $V_c$ ) were derived by subtracting the masked cone DEM (Figure 5B) from the original footprint (Figure 5A). Systematic t-test analyses ( $\alpha = 0.05$ ) were subsequently used to conduct means comparisons between cone morphology rating classes.

Table 1. Explanation of Qualitative Cone Morphology Rating

1	Good-Excellent	Cone shape with vent morphology
2	Good	Cone shape with less defined vent morphology
3	Moderate-Good	Cone shape, lacks well-defined vent morphology
4	Moderate	Cone shape, no vent
5	Moderate-Poor	Cone shape, poor definition
6	Poor	Lacks cone shape
7	Very Poor	Lacks cone shape, very poorly defined morphology

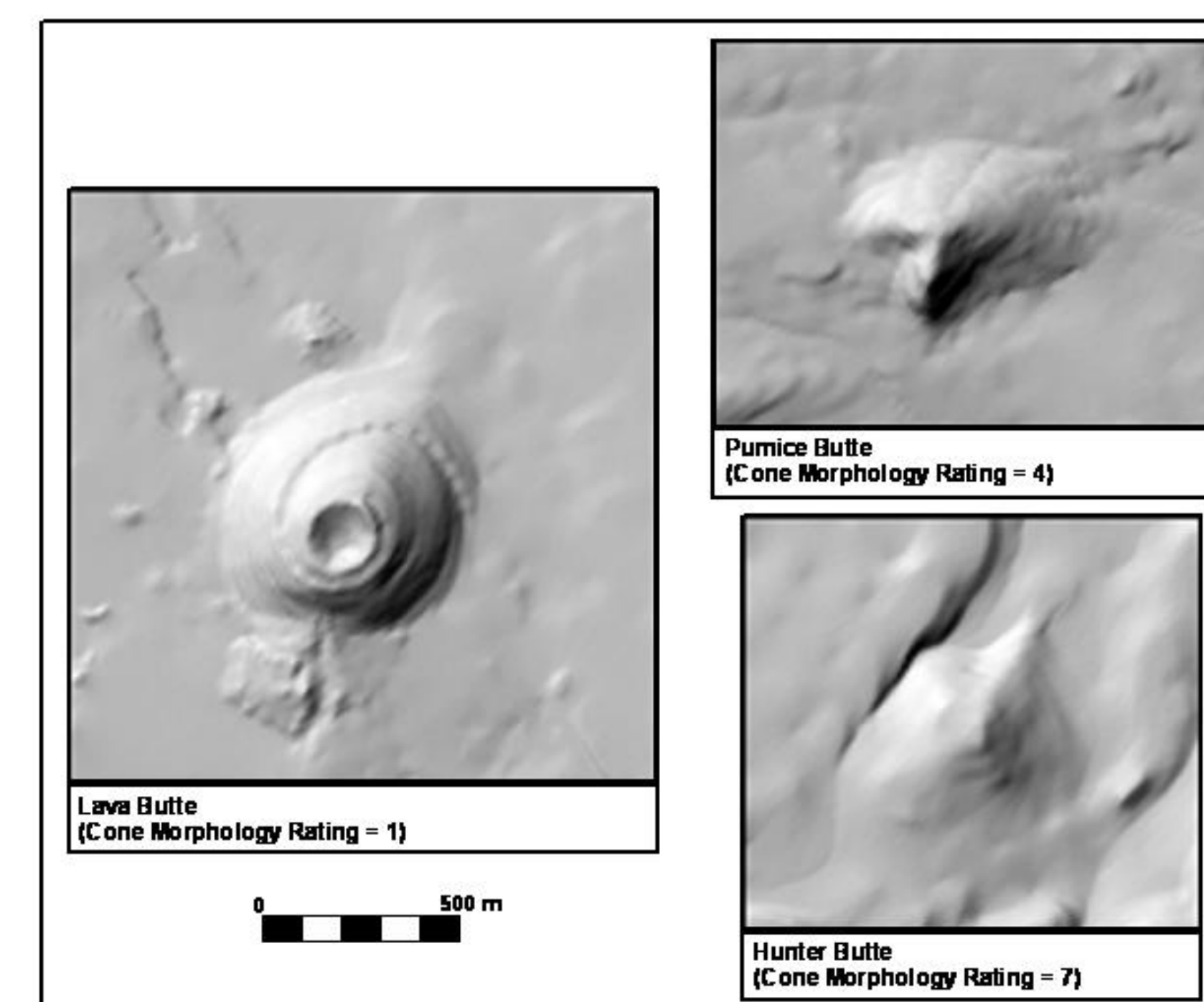


Figure 4. 10-m DEM relief maps for three select cinder cones at Newberry Volcano (map unit "C<sub>c</sub>" of MacLeod and others, 1995). Shaded relief maps were used to visually rank each cone in the data set according to qualitative appearance of shape, slope configuration, and vent morphologies (Table 1). Representative examples include Lava Butte (morphology rating = 1), Pumice Butte (morphology rating = 4), and Hunter Butte (morphology rating = 7) (Refer to Figure 6 for cone locations.)

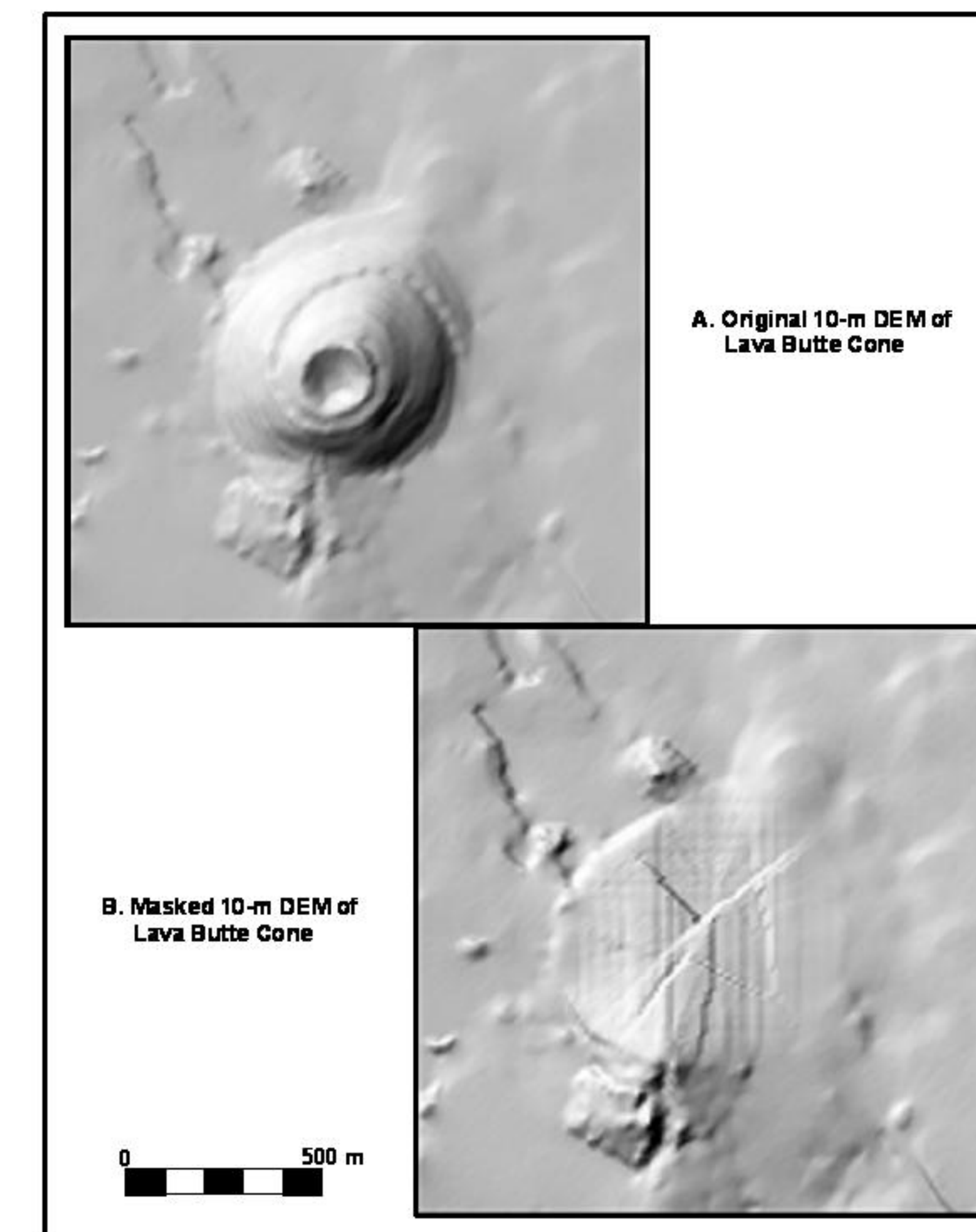


Figure 5. Shaded-relief maps illustrating the kriging-based method by which cone volumes were calculated from 10-m DEMs. Cone volumes were calculated by subtracting elevation surface B from elevation surface A above. See text for discussion.



## 5. RESULTS

### 5A. Morphometric Data

Figure 6 is a location map showing the selected Newberry cinder cones and their respective morphology ratings as described above. Morphometric results for each of the seven morphology-rating classes are listed in Table 2 and displayed in Figure 7. The results for each class are summarized as follows: (A) Frequency (no.) 1=11, 2=21, 3=10, 4=35, 5=11, 6=35, 7=59; (B) Average  $V_c$  ( $m^3$ ) 1= $1.46 \times 10^7$ , 2= $1.53 \times 10^7$ , 3= $1.25 \times 10^7$ , 4= $4.88 \times 10^6$ , 5= $4.65 \times 10^6$ , 6= $3.07 \times 10^6$ , 7= $1.10 \times 10^6$ ; (C) Average  $S_c$  (deg) 1=19.9, 2=18.2, 3=18.1, 4=14.9, 5=14.4, 6=11.9, 7=10.2; (D) Average  $H_c$  (m) 1=132, 2=124, 3=126, 4=76, 5=78, 6=59, 7=50; (E) Average  $H_c/W_c$  1=0.18, 2=0.20, 3=0.19, 4=0.15, 5=0.14, 6=0.13, 7=0.13.

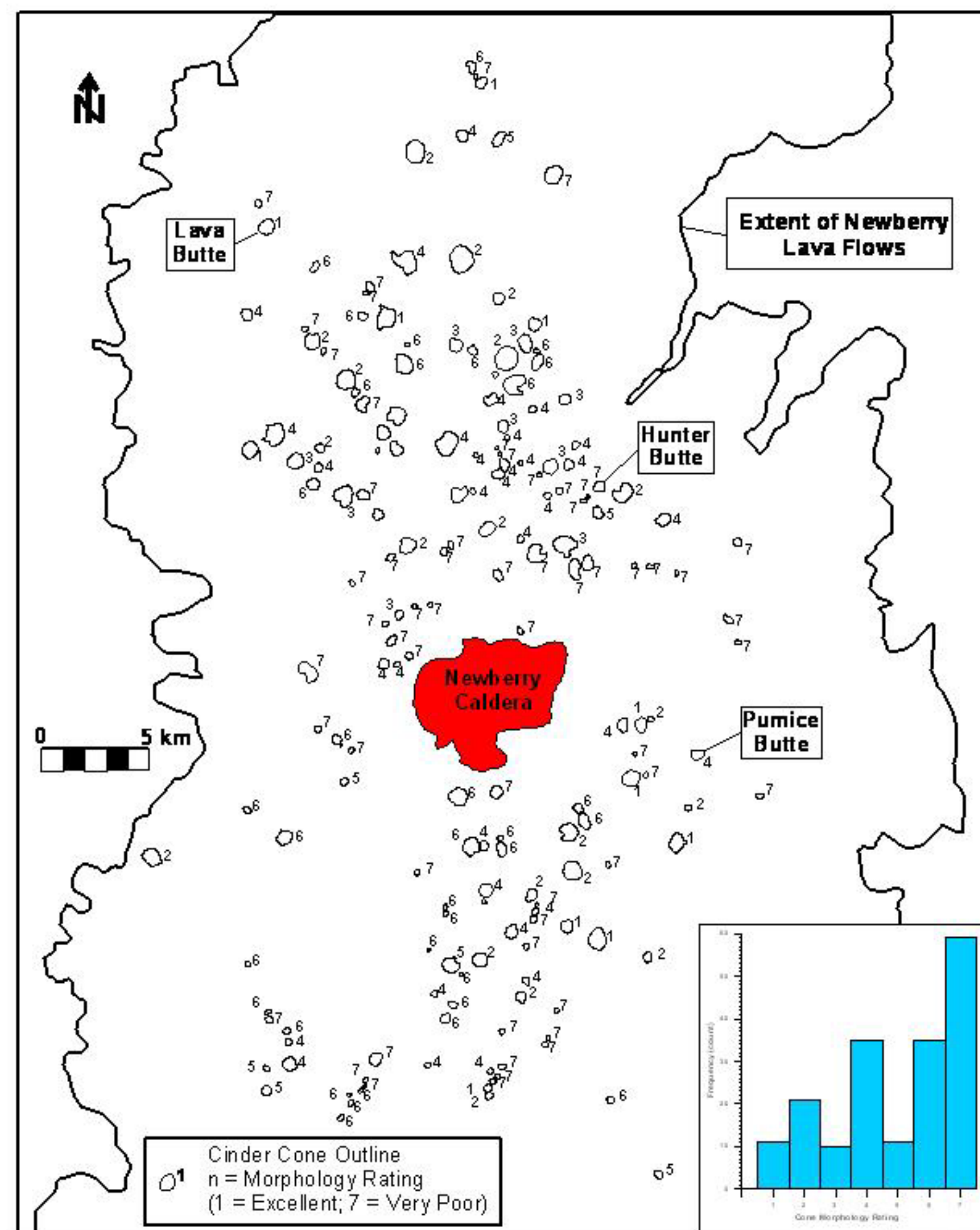


Figure 6. Map of Newberry Volcano showing outlines of single cinder cones selected for this study ( $n = 182$ ). Cone outlines were digitized from map polygon "Qc" of MacLeod and others (1995). The cone morphology rating was derived from qualitative ranking of shapes, slope configuration, and vent morphology as depicted on 10-m shaded relief maps. Inset shows morphology frequency.

Table 2. Summary of Relevant Cone Morphometry Data.

Cone Morphology Class	No.	Avg Slope (deg)		Cone Height (m)		Hco/Wco	
		Mean	Variance	Mean	Variance	Mean	Variance
Class 1	11	19.9	11.8	132.4	1344.9	0.18	0.0012
Class 2	21	18.2	10.5	124.4	2282.4	0.20	0.0073
Class 3	10	18.1	2.7	126.2	1991.0	0.19	0.0017
Class 4	35	14.9	12.1	76.2	1918.4	0.15	0.0014
Class 5	35	14.4	10.6	78.1	1682.9	0.15	0.0012
Class 6	11	11.9	13.7	59.5	1721.3	0.13	0.0025
Class 7	59	10.2	19.0	50.4	1401.3	0.14	0.0046
All Cones	182	13.6	24.2	76.4	2520.7	0.2	0.0038

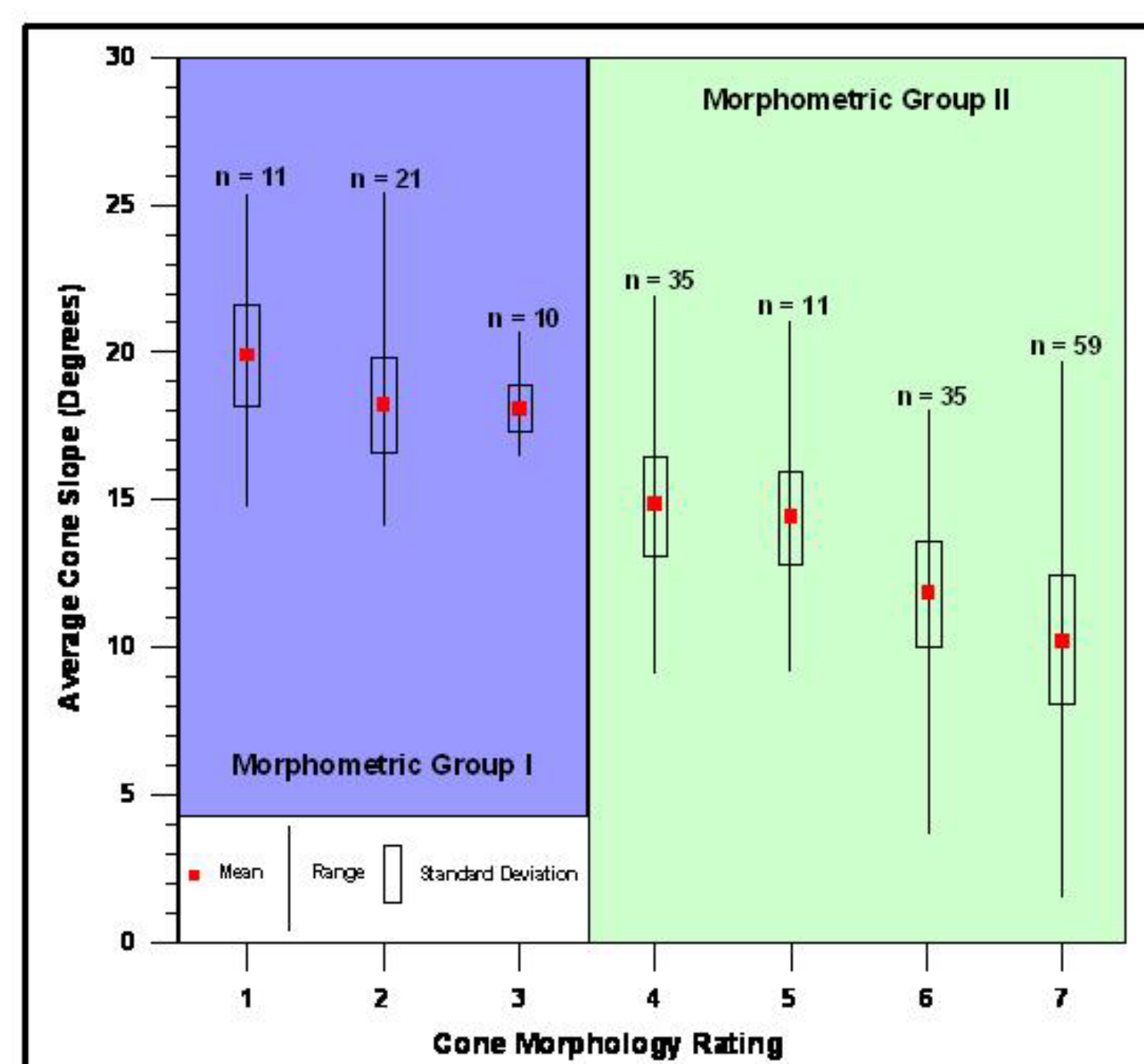


Figure 7A. Whisker plot of average cone slope (degrees) vs. qualitative cone morphology rating. Morphometric groupings are based on systematic t-test results at the 95% confidence level as summarized in Table 3.

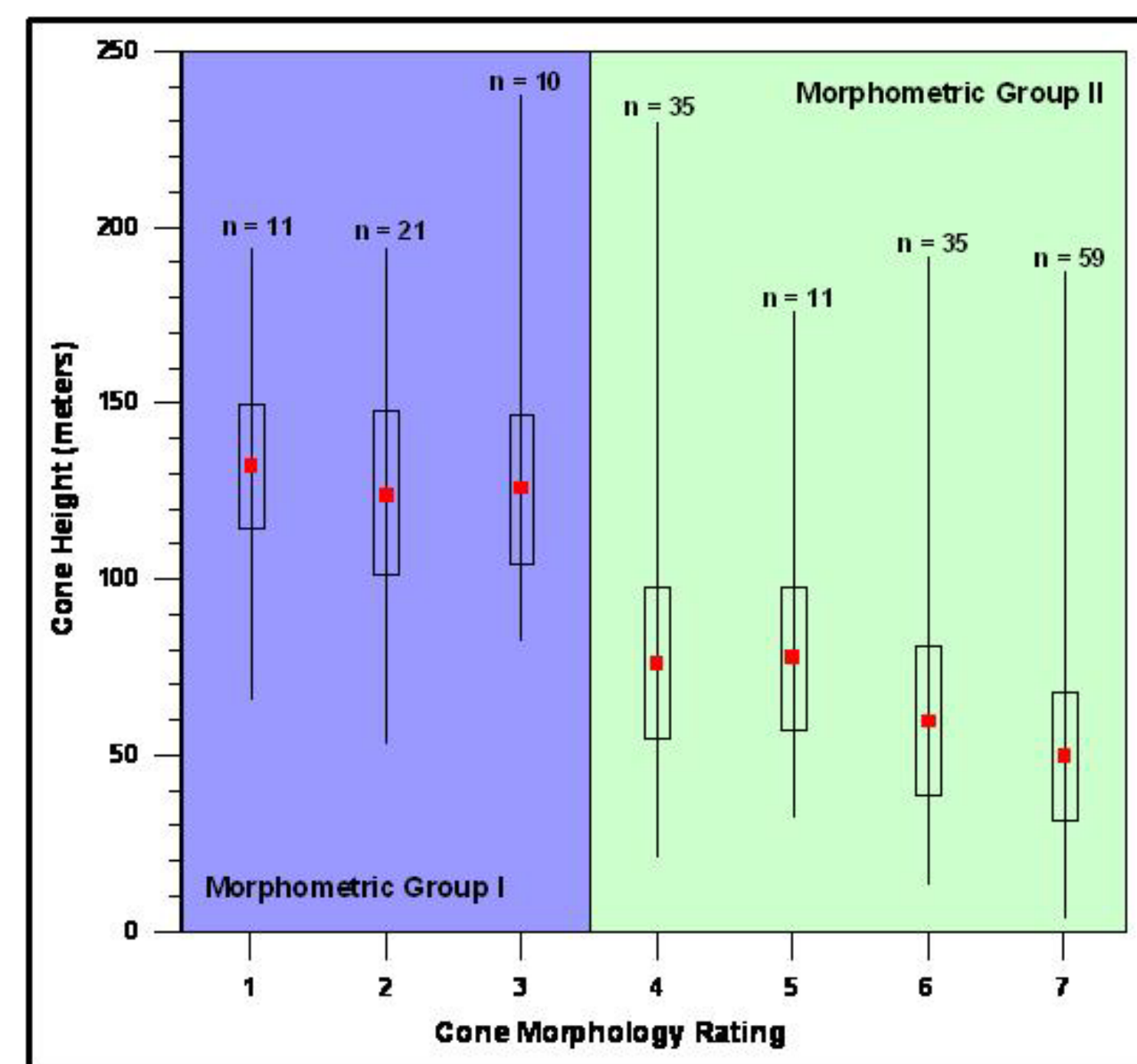


Figure 7B. Whisker plot of cone height (meters) vs. qualitative cone morphology rating. Morphometric groupings are based on systematic t-test results at the 95% confidence level as summarized in Table 3.

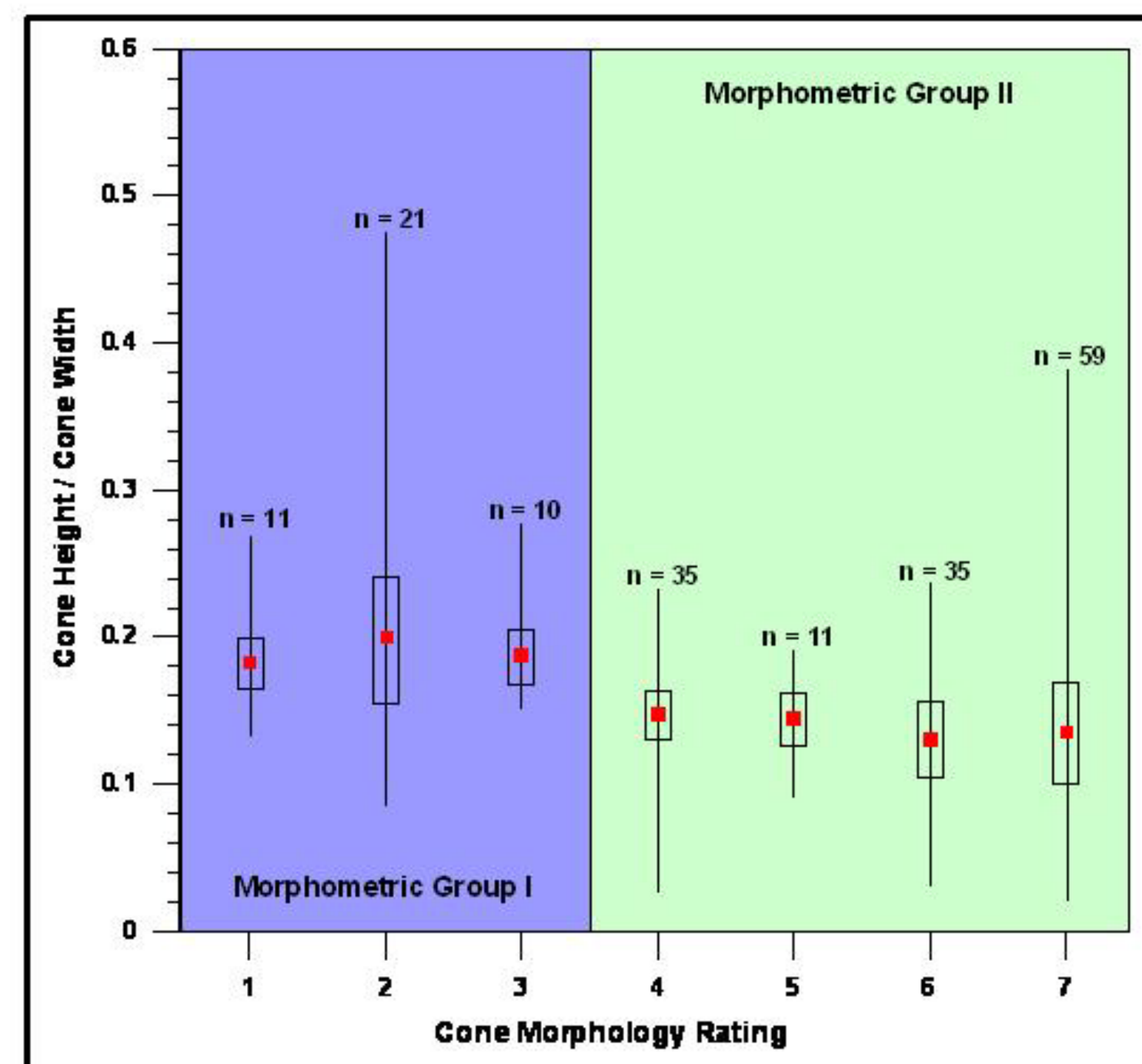


Figure 7C. Whisker plot of cone height/width ratio vs. qualitative cone morphology rating. Morphometric groupings are based on systematic t-test results at the 95% confidence level as summarized in Table 3.

### 5B. T-Test Results

Results of systematic t-tests ( $\alpha=0.05$ ) between morphology rating categories are listed in Table 3. Mean cone slope ( $S_c$ ), cone height ( $H_c$ ) and height/width ratios ( $H_c/W_c$ ) were compared to identify morphometric similarities or differences between rating categories. Systematic t-tests statistically separated cone rating categories into two groups: (1) "Morphometric Group I" = ranks 1-3, and (2) "Morphometric Group II" = ranks 4-7 (Table 3, Figure 7).

Table 3. Results of Systematic T-Test Analyses.

Cone Morphology Class	df	$\alpha$	t Stat	P(T<t) one-tail		t Critical two-tail		Test Result	Morphometric Group	
				Critical one-tail	t	Critical two-tail	t			
$S_{avg}$	Class 1-Class 2	30	0.05	1.38	0.089	1.70	0.177	2.04	Accept $H_0$	Group I
	Class 2-Class 3	29	0.05	0.11	0.458	1.70	0.915	2.05	Accept $H_0$	Group I
	Class 3-Class 4	43	0.05	2.85	0.003	1.68	0.007	2.02	Reject $H_0$	Group II
	Class 4-Class 5	44	0.05	0.36	0.360	1.68	0.719	2.02	Accept $H_0$	Group II
	Class 5-Class 6	44	0.05	2.05	0.023	1.68	0.046	2.02	Reject $H_0$	Group II
	Class 6-Class 7	92	0.05	1.88	0.032	1.66	0.064	1.99	Accept $H_0$	Group II
	Class 7-Class 8	92	0.05	1.88	0.032	1.66	0.064	1.99	Accept $H_0$	Group II
$H_c$	Class 1-Class 2	30	0.05	0.49	0.315	1.70	0.631	2.04	Accept $H_0$	Group I
	Class 2-Class 3	29	0.05	-0.10	0.459	1.70	0.918	2.05	Accept $H_0$	Group I
	Class 3-Class 4	43	0.05	3.17	0.001	1.68	0.003	2.02	Reject $H_0$	Group II
	Class 4-Class 5	44	0.05	-0.13	0.450	1.68	0.899	2.02	Accept $H_0$	Group II
	Class 5-Class 6	44	0.05	1.30	0.100	1.68	0.200	2.02	Accept $H_0$	Group II
	Class 6-Class 7	92	0.05	1.09	0.140	1.66	0.280	1.99	Accept $H_0$	Group II
	Class 7-Class 8	92	0.05	1.09	0.140	1.66	0.280	1.99	Accept $H_0$	Group II
$H_c/W_c$	Class 1-Class 2	30	0.05	-0.61	0.272	1.70	0.545	2.04	Accept $H_0$	Group I
	Class 2-Class 3	29	0.05	0.40	0.346	1.70	0.692	2.05	Accept $H_0$	Group I
	Class 3-Class 4	43	0.05	2.92	0.003	1.68	0.006	2.02	Reject $H_0$	Group II
	Class 4-Class 5	44	0.05	0.20	0.420	1.68	0.840	2.02	Accept $H_0$	Group II
	Class 5-Class 6	44	0.05	0.93	0.179	1.68	0.359	2.02	Accept $H_0$	Group II
	Class 6-Class 7	92	0.05	-0.39	0.349	1.66	0.697	1.99	Accept $H_0$	Group II
	Class 7-Class 8	92	0.05	-0.39	0.349	1.66	0.697	1.99	Accept $H_0$	Group II

### 5C. Cone Volume Analysis

Results of cone volume calculations are summarized in Table 4. Cone volumes range from  $1.97 \times 10^3 m^3$  to  $4.53 \times 10^7 m^3$ , with an average of  $5.62 \times 10^6 m^3$ . Volume data were also contoured to show spatial distribution with respect to regional structure (Figure 8). Cones with the highest volumes occur on the north flank of Newberry. Volume maxima both north and south of the summit caldera are broadly co-linear with the north-northwest trending Tumalo fault zone.

Table 4. Results of Cone Volume Calculations ( $m^3$ ).

Mean	$5.62 \times 10^6$
Median	$1.40 \times 10^6$
Mode	$7.04 \times 10^5$
Standard Deviation	$8.81 \times 10^6$
Minimum	$1.97 \times 10^3$
Maximum	$4.53 \times 10^7$
Count	177

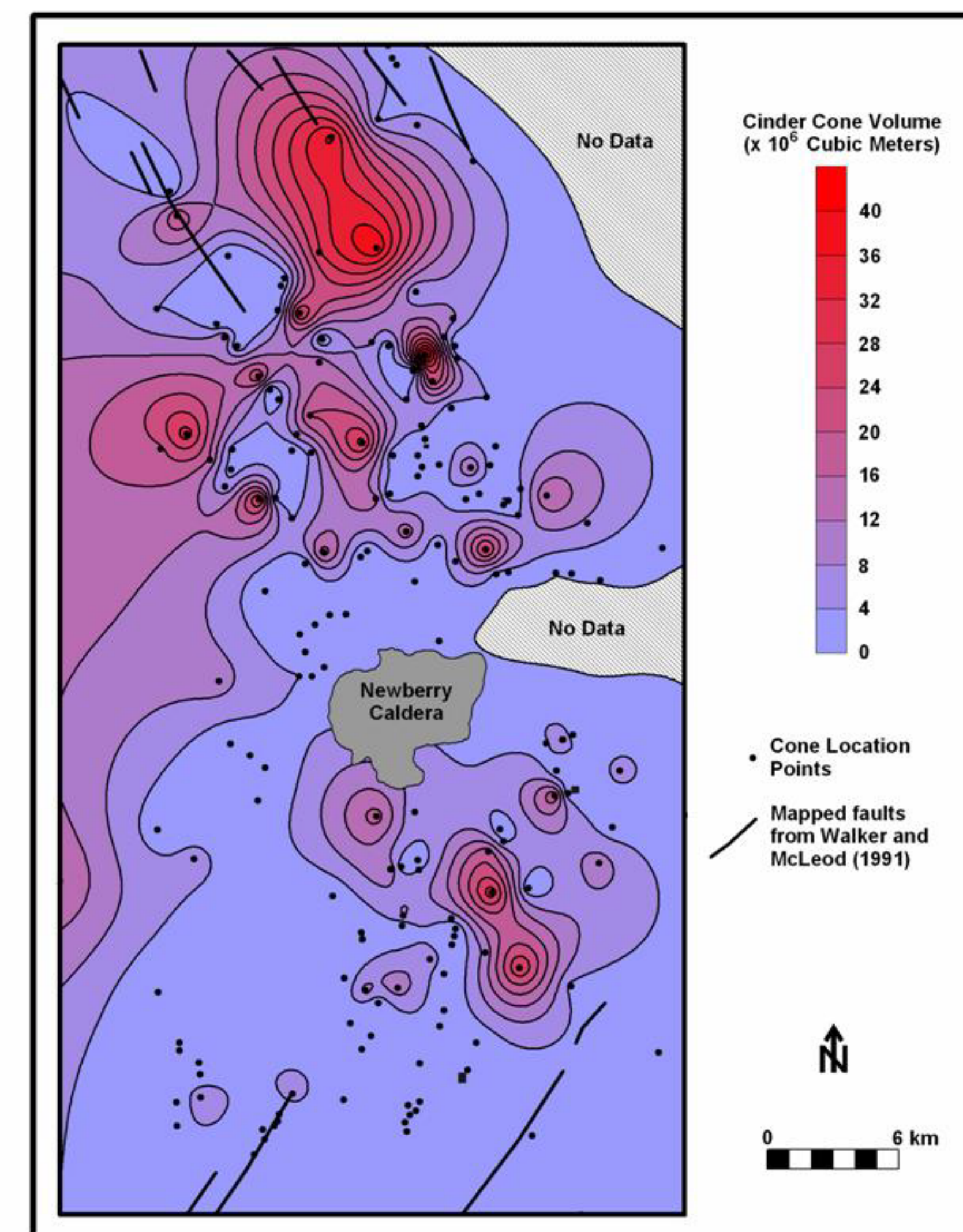


Figure 8. Contour map of select cinder cone volumes at Newberry Volcano. Note maxima oriented NW-SE, parallel to regional trend of the Tumalo fault zone.

## 6. DISCUSSION

Existing cone degradation models demonstrate that as cone age increases,  $S_c$ ,  $H_c$ , and  $H_c/W_c$  decrease, respectively (e.g. Scott and Trask, 1971; Dohrenwend and others, 1986; Hooper and Sheridan, 1998). Cones degrade over time by both diffusive and advective erosion processes, with mass transfer from hillslope to debris apron and filling of the central crater (Dohrenwend and others, 1986; Blauvelt, 1998; Rech and others, 2001). The net result is reduction of cone height and slope through time coupled with the loss of crater definition.

GIS-based analyses presented in this paper indicate that there are two distinct populations of cinder cones at Newberry. Based on comparison with similar studies, these data suggest that cones included in Morphometric Group I are relatively "young" compared to those in Group II, which are relatively "old". As such, Group I  $S_c$  and  $H_c/W_c$  values average 19-20° and 0.19, respectively, while Group II values average 11-15° and 0.14. By comparing Newberry data with age-calibrated cone morphology studies in Arizona (Hooper and Sheridan, 1998), the results imply that both Group I and

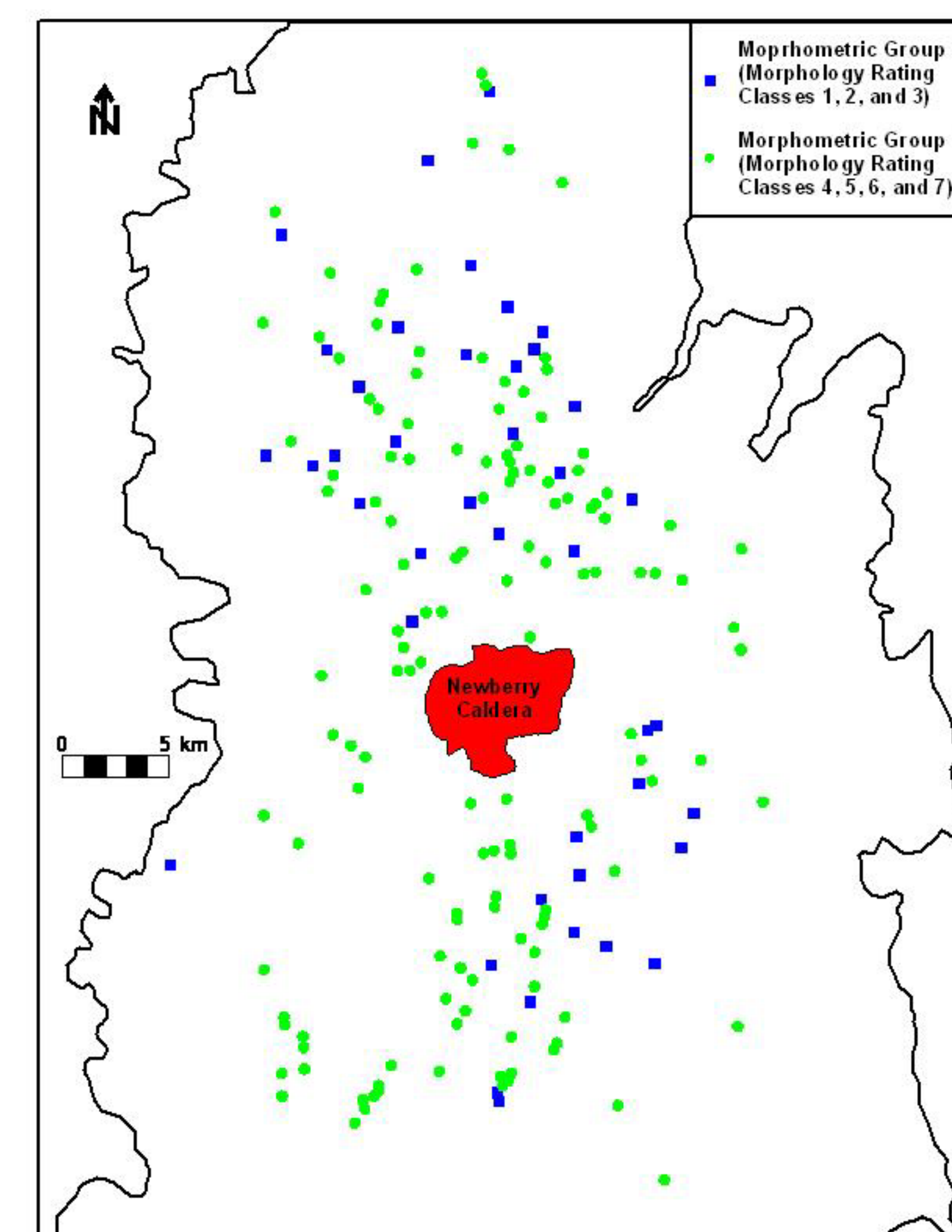


Figure 9. Map showing distribution of single cones subdivided into the two cone populations based on morphology rating. Group 1 cones consist of morphology rating classes 1, 2, and 3, and Group 2 cones consist of morphology rating classes 4, 5, 6, and 7.

Group II cones fall within a "Holocene-Latest Pleistocene" age category. However, higher resolution chronometry is required to more definitively establish age trends in the cones selected for this study. Based on preliminary comparison with dated eruptive events at Newberry (Jensen, 2000), it is uncertain if the morphometric groupings delineated in this study are a function of age differences (i.e. degradational processes) or a combination of other variables such as climate, post-eruption cone burial, lava composition, and episodic ("polygenetic") eruption cycles. Further radiometric and geomorphic dating studies will be required to definitively decipher the factors controlling the two morphometric groupings identified in this work.

Cone clustering and alignment patterns are commonly recognized at volcanic fields (Porter, 1972; Settle, 1979; Connor, 1990). Spatial-distribution patterns of Newberry morphometric groups (Figure 9) shows a northwest-southeast alignment of Group I cones and a northeast-southwest alignment of some Group II cones. While care must be taken when inferring linear trends from cinder cone arrays, these data lend support to the hypothesis of MacLeod and Sherrod (1988) that north-northwest trending clusters are relatively younger than those oriented north-northeast. Regional and local tectonic stress fields are often interpreted as the primary factor controlling such cone distribution patterns. Parallel alignment of Newberry cone-volume maxima with the Tumalo fault zone implies that this structure has an important control on eruptive processes. This observation supports the contention of MacLeod and Sherrod (1988) that faulting and regional tectonic stress fields structurally control mafic eruptions at Newberry.

## 7. CONCLUSION

Morphometric and volume-distribution analyses of cinder cones at Newberry Volcano suggest that cones are systematically organized in both space and time. Two morphometric groupings of cinder cones are statistically recognized at the 95% confidence level. Possible controlling factors include degradation processes, age differences, climate, post-eruption cone burial, lava composition, and episodic ("polygenetic") eruption cycles. Parallel alignment of cone-volume maxima with known fault trends implies that these structures have an important control on eruptive processes in the region. This study provides a preliminary framework to guide future geomorphic analyses and radiometric age dating of Newberry cinder cones.

## 8. ACKNOWLEDGMENTS

Work on this project was initially stimulated by group discussions related to the Fall 2000 Friends of the Pleistocene, Pacific Northwest Cell, field trip to Newberry Volcano. Special thanks are extended to the FOP organizers and presenters for elucidating many of the interesting research problems associated with Newberry. Portions of this study were funded by the College of Liberal Arts and Sciences, the Faculty Development Grant Program, the ASWOU Student Technology Fee Committee, and the PT3 Project at Western Oregon University. Tony Faletti, Diane Horvath, Diane Hale, and Ryan Adams are also acknowledged as exemplary WOU Earth Science students who assisted with the tedious task of map digitization.

## 9. REFERENCES CITED

- Bacon, C.R., 1983. Eruptive history of Mount Mazama, Cascade Range, U.S.A.: Journal of Volcanology and Geothermal Research, v. 18, p. 97-115.
- Blauvelt, D.J., 1998. Examples of scoria cone degradation in the San Francisco volcanic field, Arizona. M.S. Thesis, State University of New York at Buffalo, Amherst, NY, 127 p.
- Chitwood, L.A., 2000. Geologic overview of Newberry Volcano, in Jensen, R.A., and Chitwood, L.A., eds., What's New at Newberry Volcano, Oregon: Guidebook for the Friends of the Pleistocene Eighth Annual Pacific Northwest Cell Field Trip, p. 27-30.
- Connor, C.B., 1990. Cinder cone clustering in the TransMexican Volcanic Belt: Implications for structural and petrologic models. Journal of Geophysical Research, v. 95, p. 19,395-19,405.
- Dohrenwend, J.C., Wells, S.G., and Turin, B.D., 1986. Degradation of Quaternary cinder cones in the Crima volcanic field, Mojave Desert, California. Geological Society of America Bulletin, v. 97, p. 421-427.
- Giles, D.E., Taylor, S.B., and Templeton, J.H., 2003. Compilation of a digital geologic map and spatial database for Newberry volcano, central Oregon: A framework for comparative analysis. Geological Society of America Abstracts with Programs, v. 35, no. 6, p. 189.
- Higgins, M.V., 1973. Petrology of Newberry Volcano, Central Oregon. Geological Society of America Bulletin, v. 84, p. 455-488.
- Hooper, D.M., and Sheridan, M.F., 1998. Computer-simulation models of scoria cone degradation. Journal of Volcanology and Geothermal Research, v. 83, p. 241-267.
- Jensen, R.A., 2000. Roadside Guide to the Geology of Newberry Volcano, 3rd ed. CenOreGeoPub, Bend, Oregon, 168 pp.
- Jensen, R.A., and Chitwood, L.A., 2000. Geologic overview of Newberry Volcano, in Jensen, R.A., and Chitwood, L.A., eds., What's New at Newberry Volcano, Oregon: Guidebook for the Friends of the Pleistocene Eighth Annual Pacific Northwest Cell Field Trip, p. 27-30.
- MacLeod, N.S., and Sherrod, D.R., 1988. Geologic evidence for a magma chamber beneath Newberry Volcano, Oregon. Journal of Geophysical Research, v. 93, p. 10,067-10,079.
- MacLeod, N.S., Sherrod, D.R., Chitwood, L.A., and McKee, E.H., 1981. Newberry Volcano, Oregon, in Johnston, D.A., and Donnelly-Nolan, J., eds., Guides to some volcanic terranes in Washington, Idaho, and northern California: U.S. Geological Survey Circular 838, p. 85-103.
- MacLeod, N.S., Sherrod, D.R., Chitwood, L.A., and Jensen, R.A., 1995. Geologic Map of Newberry Volcano, Deschutes, Klamath, and Lake Counties, Oregon: U.S. Geological Survey Miscellaneous Geologic Investigations Map I-2455, scales: 1:62,500 and 1:24,000.
- Porter, S.C., 1972. Distribution, morphology, and size frequency of cinder cones on Mauna Kea volcano, Hawaii. Geological Society of America Bulletin, v. 83, p. 3607-3612.
- Rech, J.A., Reeves, R.W., and Hendricks, D.M., 2001. The influence of slope aspect on soil weathering processes in the Springerville volcanic field, Arizona. Catena, v. 43, p. 49-62.
- Scott, D.H., and Trask, N.J., 1971. Geology of the Lunar Crater volcanic field, Nye County, NV. U.S. Geological Survey Professional Paper, 599-1, 22 p.
- Settle, M., 1979. The structure and emplacement of cinder cone fields. American Journal of Science, v. 279, p. 1089-1107.
- Sherrod, D.R., Mastin, L.G., Scott, W.E., and Schilling, S.P., 1997. Volcano hazards at Newberry Volcano, Oregon. U.S. Geological Survey, Open-file Report 97-513, 14 pp.
- U.S. Census Bureau, 2003. Census data for the state of Oregon: online resource, <http://www.census.gov>.
- Walker, G.W., and MacLeod, N.S., 1991. Geologic Map of Oregon: U.S. Geological Survey, Scale, 1:500,000.
- Wood, C.A., 1980. Morphometric evolution of cinder cones. Journal of Volcanology and Geothermal Research, v. 7, p. 387-413.